Laser and Particle Beams

cambridge.org/lpb

Transverse electromagnetic Hermite–Gaussian mode-driven direct laser acceleration of electron under the influence of axial magnetic field

Harjit Singh Ghotra[1], Dino Jaroszynski[2], Bernhard Ersfeld[2], Nareshpal Singh Saini[3], Samuel Yoffe[2] and Niti Kant[1]

[1]Department of Physics, Lovely Professional University, G. T. Road, Phagwara-144411, Punjab, India; [2]Scottish Universities Physics Alliance (SUPA), University of Strathclyde, Glasgow G4 0NG, Scotland, UK and [3]Department of Physics, Guru Nanak Dev University, Amritsar-143005, Punjab, India

Research Article

Cite this article: Ghotra HS, Jaroszynski D, Ersfeld B, Saini NS, Yoffe S, Kant N (2018). Transverse electromagnetic Hermite–Gaussian mode-driven direct laser acceleration of electron under the influence of axial magnetic field. *Laser and Particle Beams* **36**, 154–161. https://doi.org/10.1017/S0263034618000083

Received: 12 November 2017
Revised: 19 February 2018
Accepted: 20 February 2018

Key words:
Axial magnetic field; electron acceleration; Hermite–Gaussian laser; TEM modes; vacuum

Author for correspondence:
Niti Kant, Department of Physics, Lovely Professional University, G. T. Road, Phagwara-144411, Punjab, India,
E-mail: nitikant@yahoo.com

Abstract

Hermite–Gaussian (HG) laser beam with transverse electromagnetic (TEM) mode indices (m, n) of distinct values (0, 1), (0, 2), (0, 3), and (0, 4) has been analyzed theoretically for direct laser acceleration (DLA) of electron under the influence of an externally applied axial magnetic field. The propagation characteristics of a TEM HG beam in vacuum control the dynamics of electron during laser–electron interaction. The applied magnetic field strengthens the $\vec{v} \times \vec{B}$ force component of the fields acting on electron for the occurrence of strong betatron resonance. An axially confined enhanced acceleration is observed due to axial magnetic field. The electron energy gain is sensitive not only to mode indices of TEM HG laser beam but also to applied magnetic field. Higher energy gain in GeV range is seen with higher mode indices in the presence of applied magnetic field. The obtained results with distinct TEM modes would be helpful in the development of better table top accelerators of diverse needs.

Introduction

The charged particle trapping and accelerating with a laser field is a fascinating concept since last few decades (Tajima & Dawson, 1979; Sprangle *et al.*, 1996; Umstadter, 2003). The rising interests to accelerate electron with a high energy remain a motivation for the investigation and development of advanced electron acceleration techniques (Leemans *et al.*, 2006; Ghotra & Kant, 2015*a*). Several theoretical and experimental models are proposed by various researchers that report an effective energy gained by the electron during interaction with ultra-short and intense laser pulse (Geddes *et al.*, 2004; Joshi, 2007; Malka *et al.*, 2008; Ghotra & Kant, 2015*b*; Albert *et al.*, 2017; Mohammed *et al.*, 2017; Wallin *et al.*, 2017). The energy gained by the electron is sensitive to laser's power, beam waist, and pulse duration (Ghotra & Kant, 2017; Fortin *et al.*, 2010). Laser–plasma interactions indicate that there is a generation of superponderomotive electrons due to a non-wake-field interaction between a laser pulse and a longitudinal electric field (Robinson *et al.*, 2013). There appears a dephasing that reduces the electron acceleration. The longitudinal electric field acts as an extra field that could reduce the dephasing rate for an efficient acceleration. Vacuum-based acceleration of electron has some advantages over plasma as it presents a greater group velocity of a laser pulse, and also the plasma-related instabilities are absent in vacuum, which appears as a better option for laser–electron interaction. Further, it is much easier to inject a pre-accelerated electron in vacuum than in plasma. Gaussian laser fields with appropriate profiles prove their suitability for effective acceleration of electron because of their ability of achieving a high energy with restricted spread and small divergence of electron beams (Fortin *et al.*, 2010). The Gaussian laser beam fields and their propagation properties are dependent on laser beam frequency ω, intensity parameter a_0, beam waist radius r_0 at the focus, pulse duration τ and Rayleigh length $Z_R = kr_0^2/2$. A few MeV of electron energy gain was observed with intensity above $10^{19}\mathrm{W/cm^2}$ with a Gaussian laser beam (Ghotra & Kant, 2016*a*). The parameters such as external magnetic field, frequency variations and polarization characteristics of laser pulse influence the electron dynamics, and hence the electron energy gain (Ghotra & Kant, 2016*a*; Salamin, 2017). The transverse electromagnetic (TEM) mode index-driven intensity variations of electromagnetic fields were investigated with intense laser beams (Kawata *et al.*, 2005; Gu *et al.*, 2016; Ghotra & Kant, 2016*b*). Beam that involves a product of Hermite with Gaussian functions configures Hermite–Gaussian (HG) beam. The propagation characteristics of HG beam can be expressed in terms of different modes and represented as

CAMBRIDGE UNIVERSITY PRESS

TEM_{mn}, where m and n correspond to the mode indices. The lowest order mode (TEM_{00}) of such beam represents a Gaussian beam. An experiment was conducted using HG laser beam with distinct modes (0, 0), (0, 1), (0, 2), (0, 3), and (0, 4) to investigate the emergence of mega gauss ordered persisting magnetic field due to relativistic electrons in plasma (Flacco *et al.*, 2015). The polarization characteristics of a Gaussian laser beam indicate higher energy gain by the electron with a circularly polarized (CP) laser beam in comparison with a linearly polarized (LP) laser beam. The accelerated electron disperses with a low energy for a Gaussian TEM_{00} mode due to a strong transverse ponderomotive force. However, for an effective acceleration, the externally applied inhomogeneous magnetic field ensures a better trapping of electron near the focus of Gaussian laser pulse with TEM_{00} mode (Saberi & Maraghechi, 2015). The HG beam with its higher modes enforces a better confining of electron close to its focus axis with TEM_{00} mode due to their characteristics intensity distributions. The electron acceleration under the influence of TEM modes of HG laser beam was investigated, which depicts that a lower mode indexed HG laser beam enforces a small acceleration of electron for longer distance, whereas, a higher mode indexed HG laser beam enforces a larger acceleration of electron for smaller distance without application of any external magnetic field (Ghotra & Kant, 2016*b*). The detrimental effect of the B-fields on electron and ion acceleration has been evoked in an experimental and simulation study (Nakatsutsumi *et al.*, 2018). The inductive generation of the B-field is mainly determined by the spatio-temporal variations of the longitudinal sheath field: $\partial B_z/\partial t = \partial E_x/\partial t$. Those fields can be strong enough ($\sim 10^5$ T at laser intensities $\sim 10^{21}$ W cm^{-2}) to magnetize the sheath electrons and deflect protons off the accelerating region, hence degrading the maximum energy. Such spatiotemporal-restricted magnetic field has larger impact on electron acceleration in plasma. The effect can be neglected for the case of direct laser acceleration (DLA) of electron in vacuum.

In this manuscript, an external axial magnetic field is employed to analyze the effect of distinct TEM modes of Hermite function on DLA of electron with a relativistic three-dimensional single-particle code using a CP Gaussian laser beam. Electron acceleration is shown to be influenced by the beam width parameter, propagation distance in terms of Rayleigh length, laser spot size, mode indices, and applied magnetic field. The influence of laser beam width parameter has been investigated on electron acceleration with distinct values of laser intensity and externally applied axial magnetic field in vacuum. The energy gained by the electron for distinct TEM modes (0, 1), (0, 2), and (0, 3) with respect to propagation distance has been analyzed without and with axial magnetic field. The acceleration distance is expressed in terms of Rayleigh length for distinct mode indices. The external magnetic field plays a vital role in controlling the electron dynamics. It strengthens the $\vec{v} \times \vec{B}$ force component of the fields for the occurrence of strong betatron resonance, which enhances electron oscillations. Hence, it ensures the confining of electron in close orbit around the axis of propagation of laser pulse. With lower mode index, the electron's acceleration remains small and focused toward the axis, the external magnetic field enhances the acceleration, and hence electron energy gain by confining the oscillations. However, with higher mode index where electron appears with larger acceleration for smaller distance, the magnetic field ensures the confining of electron around the axis for larger accelerating distance with enhanced energy gain. Presented results of electron energy gain with propagation distance under the influence of suitable magnetic field may be helpful in the development of better table-top electron accelerators of diverse dimensions and capabilities. The role of distinct mode indices and external magnetic field can be utilized for the formulation of desired-sized accelerators based on the accelerating distance of electron. The content in other sections of this paper is organized as follows. Section "Evolution of CP–HG beam" describes about the field distributions of a CP–HG laser beam, section "Relativistic analysis based on electron dynamics" describes the electron dynamics to relate the electron acceleration during interaction with laser and external fields. Outcomes are explained in section "Results and discussion". Lastly, a conclusion is drawn and presented in section "Conclusion".

Evolution of CP–HG beam

A CP–HG laser beam is considered to be propagating in the z-direction. Under paraxial approximation, the transverse electric field components can be expressed as (Kawata *et al.*, 2005; Gu *et al.*, 2016):

$$E_x(r,z,t) = \frac{E_0}{f(\xi)} \exp(i\phi) H_m\left(\frac{\sqrt{2}}{r_0 f(\xi)} x\right) \times \exp\left(-\frac{(t-((z-z_L)/c))^2}{\tau^2} - \frac{r^2}{r_0^2 f^2}\right), \quad (1)$$

$$E_y(r,z,t) = \frac{E_0}{f(\xi)} \exp\left[i\left(\phi + \frac{\pi}{2}\right)\right] H_n\left(\frac{\sqrt{2}}{r_0 f(\xi)} y\right) \times \exp\left(-\frac{(t-((z-z_L)/c))^2}{\tau^2} - \frac{r^2}{r_0^2 f^2}\right), \quad (2)$$

where E_0 and ϕ are the field amplitude and phase of HG laser beam, respectively; m, n represent the indices of a Hermite-polynomial $H_{m,n}$ function; τ and r_0 are the laser's pulse duration and spot size, respectively; $r^2 = x^2 + y^2$, z_L is the initial pulse peak position; and c is the speed of light in vacuum. The beam width parameter of laser is expressed in terms of function $f(\xi)$ as:

$$f(\xi) = \sqrt{1+\xi^2}, \quad (3)$$

where $\xi = z/Z_R$ is the propagation distance normalized in terms of Rayleigh length $Z_R = kr_0^2/2$, k and ω_0 are the laser's wave number and frequency, respectively, $\phi = \omega_0 t - kz + (n+m+1)\tan^{-1}(\xi) - r^2 z/(Z_R r_0^2 f^2) + \phi_0$, hence $(n+m+1)\tan^{-1}(\xi)$ expresses the Guoy phase, and ϕ_0 is the initial phase.

The longitudinal components of the electric and magnetic fields are expressed by paraxial ray approximation as:

$$E_z(r,z,t) = -\left(\frac{i}{k}\right)\left(\frac{\partial E_x}{\partial x} + \frac{\partial E_y}{\partial y}\right), \quad (4)$$

$$\vec{B}(r,z,t) = -\left(\frac{i}{\omega}\right)(\vec{\nabla} \times \vec{E}). \quad (5)$$

The amplitude of the longitudinal laser field in vacuum is only about $0.03E_0$ for a Gaussian laser beam (Xiao *et al.*, 2016)

https://doi.org/10.1017/S0263034618000083 Published online by Cambridge University Press

indicating a very small longitudinal laser field in comparison with transverse components. In our presented equation (4), the longitudinal electric field component is smaller by a factor of $(1/k)$ as compared with transverse field components. Thus, the contribution of longitudinal electric field component in our model is very small for DLA of electron in comparison with transverse component in vacuum.

The externally applied axial magnetic field is in longitudinal direction of laser pulse. Such axial magnetic field is expressed as (Ghotra & Kant, 2017):

$$\vec{B} = B_0 \hat{z}, \tag{6}$$

where B_0 is the magnetic field amplitude.

Relativistic analysis based on electron dynamics

The relativistic equations governing the momentum and energy of the accelerated electron in consideration of externally applied axial magnetic field are expressed as:

$$\frac{dp_x}{dt} = -eE_x + e\beta_z B_y - e\beta_y (B_z + B_0), \tag{7}$$

$$\frac{dp_y}{dt} = -eE_y - e\beta_z B_x + e\beta_x (B_z + B_0), \tag{8}$$

$$\frac{dp_z}{dt} = -eE_z - e(\beta_x B_y - \beta_y B_x), \tag{9}$$

$$\frac{d\gamma}{dt} = -e(\beta_x E_x + \beta_y E_y + \beta_z E_z). \tag{10}$$

where $p_{x,y,z}$ represents the momentum coordinates and $\vec{p} = \gamma m_0 \vec{v}$; $\beta_{x,y,z}$ represents the normalized velocity coordinates and $\vec{\beta} = \vec{v}/c$; $\gamma^2 = 1 + (p_x^2 + p_y^2 + p_z^2)/(m_0 c)^2$ is the Lorentz factor; $-e$ and m_0 are the charge and rest mass of the electron. The other used parameters are normalized as follow:

$$a_0 \to \frac{eE_0}{m_0 \omega_0 c},\ \tau' \to \omega_0 \tau,\ r_0' \to \frac{\omega_0 r_0}{c},\ z_L' \to \frac{\omega_0 z_L}{c},\ x' \to \frac{\omega_0 x}{c},\ y' \to \frac{\omega_0 y}{c},\ z' \to \frac{\omega_0 z}{c},$$

$$\beta_x \to \frac{v_x}{c},\ \beta_y \to \frac{v_y}{c},\ \beta_z \to \frac{v_z}{c},\ t' \to \omega_0 t,\ p_0' \to \frac{p_0}{m_0 c},\ p_x' \to \frac{p_x}{m_0 c},\ p_y' \to \frac{p_y}{m_0 c},$$

$$p_z' \to \frac{p_z}{m_0 c},\ k' \to \frac{ck}{\omega_0} \text{ and } b_0 \to \frac{eB_0}{m_0 \omega_0 c}.$$

The coupled differential equations (7)–(10) with all normalized parameters have been solved numerically with a computer programing for the electron dynamics and electron energy gain.

The electron is assumed to be pre-accelerated and injected initially at a small angle δ with respect to the laser propagation axis with momentum (Ghotra & Kant, 2015*a*, *b*):

$$\vec{p_0} = \hat{x} p_0 \sin\delta + \hat{z} p_0 \cos\delta, \tag{11}$$

where p_0 is the initial momentum of the injected electron.

Results and discussion

The numerical analysis is based on the following dimensionless parameters: $a_0 = 5$ (represents laser intensity $I \sim 6.92 \times 10^{19}\text{W/cm}^2$), $a_0 = 25$ ($I \sim 8.5 \times 10^{20}\text{W/cm}^2$), $a_0 = 50$ ($I \sim 6.8 \times 10^{21}\text{W/cm}^2$); $r'_0 = 150$ (represents laser spot size $r_0 \sim 25\mu\text{m}$), $r'_0 = 300$ ($r_0 \sim 50\mu\text{m}$), $r'_0 = 450$ ($r_0 \sim 75\mu\text{m}$), $\tau'_L = 70$ (represents laser pulse duration $\tau_L = 200\text{fs}$); $z'_L = 0$; initially the electron is at $x'_i = 0$, $y'_i = 0$, and $z'_i = 0$; initial phase $\phi_0 = 0$, and $b_0 = 0.006$ (represents magnetic field of 0.64MG), b = 0.06 (~6.4MG); $\delta = 10^\circ$ and $p'_0 = 1$. The laser pulse peak power is about 0.67PW, which corresponds to intensity parameter $a_0 = 5$ with $r'_0 = 150$. In the present scenario, the laser pulse peak power in the range of PW is feasible and observed experimentally (Spinka & Haefner, 2017; Dabu, 2017).

In Figure 1, the electron energy gain is analyzed as a function of normalized axial magnetic field b_0 for the mode index $(m, n) = (0, 1)$ with normalized intensity parameter $a_0 = 5$ and 25 for

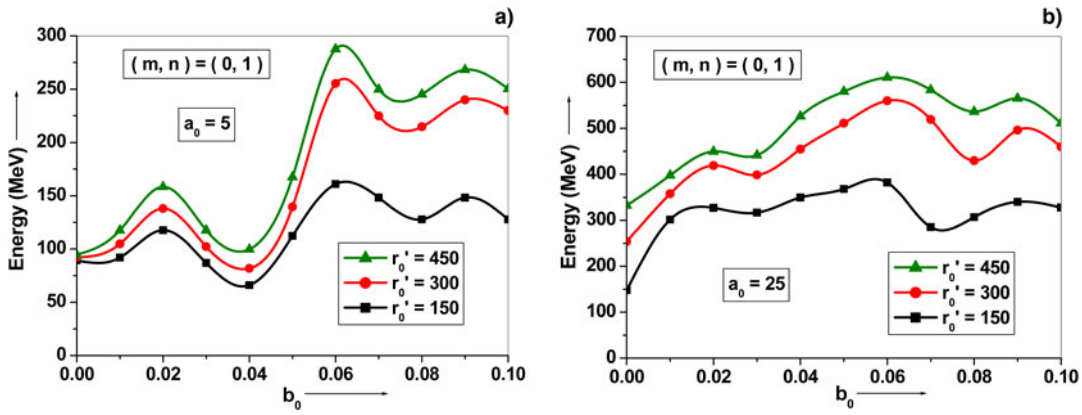

Fig. 1. Evolution of electron energy gain with a normalized function of axial magnetic field b_0 for a TEM CP–HG laser pulse with mode index $(m, n) = (0, 1)$, for different values of laser spot sizes $r'_0 = 150$, 300, and 450 at (a) $a_0 = 5$ and (b) $a_0 = 25$. The other used parameters are $\phi_0 = 0$ and $\tau'_L = 70$.

https://doi.org/10.1017/S0263034618000083 Published online by Cambridge University Press

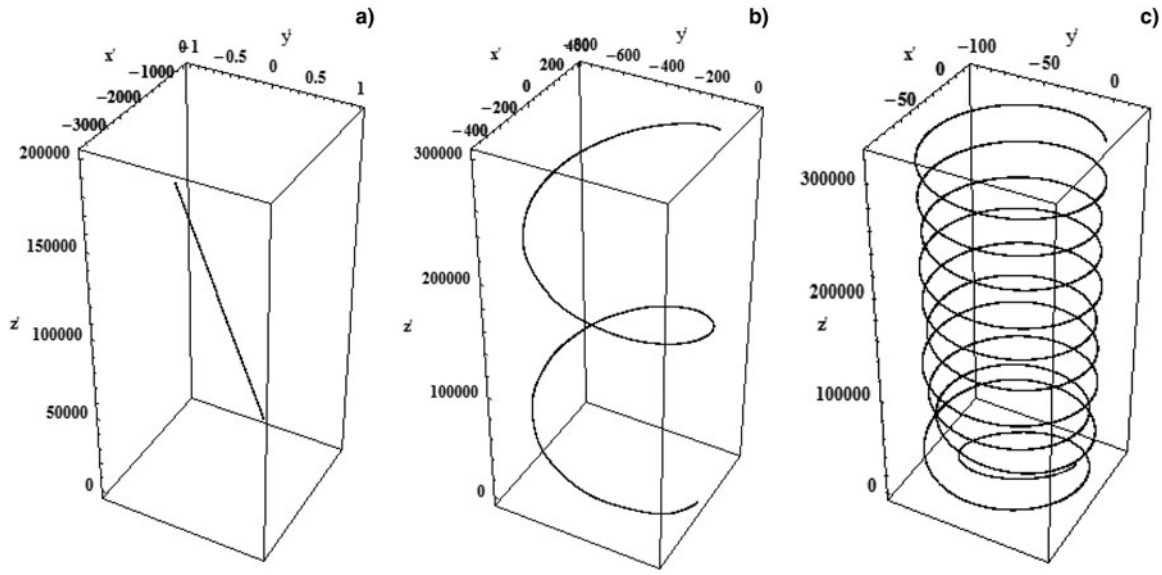

Fig. 2. Three-dimensional plots for electron trajectory without and with applied axial magnetic field for a TEM CP–HG laser pulse with mode index $(m, n) = (0, 1)$ for $a_0 = 5$ with (a) $b_0 = 0$, (b) $b_0 = 0.006$, and (c) $b_0 = 0.06$. The other parameters are $r'_0 = 150$, $\phi_0 = 0$, and $\tau'_L = 70$.

different values of normalized laser spot size $r'_0 = 150$, 300 and 450. The higher energy gain is depicted at the optimized value of magnetic field, which determines the resonance to maximize the electron energy gain. The magnetic field determines the cyclotron resonance for electron acceleration by laser in vacuum. The magnetic field determines the cyclotron resonance for electron acceleration by a laser beam in vacuum. For a TEM HG mode laser beam, the phase velocity v_{ph} is different for different TEM mode indices making resonant frequency different with different modes. Resonance occurs when the laser frequency ω_L coincides

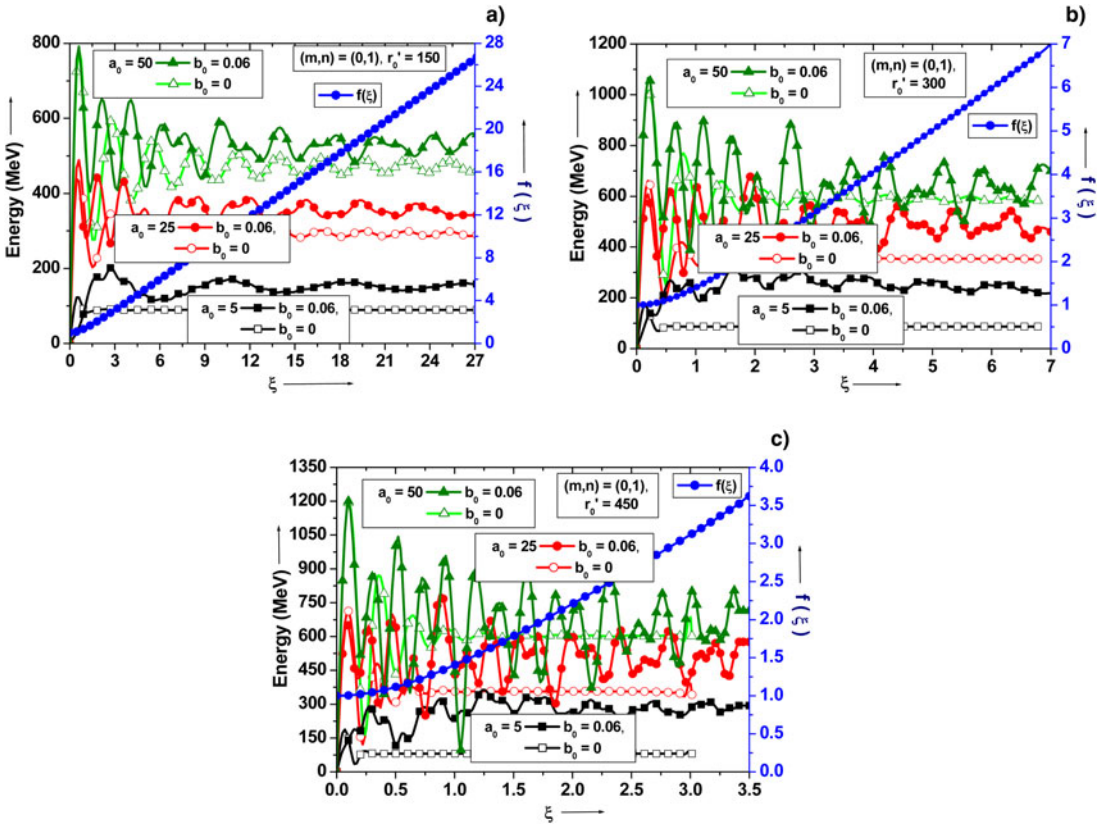

Fig. 3. Electron energy gain variations for $(m, n) = (0, 1)$ with a normalized function of propagation distance ξ and laser beam width parameter $f(\xi)$ with $b_0 = 0$ and $b_0 = 0.06$ for the different values of intensity parameter $a_0 = 5$, 25, and 50 for (a) $r'_0 = 150$, (b) $r'_0 = 300$, and (c) $r'_0 = 450$. The other parameters are $\tau'_L = 70$, $\phi_0 = 0$, $p'_0 = 1$, $z'_L = 0$, $x'_i = 0$, $y'_i = 0$, and $z'_i = 0$.

https://doi.org/10.1017/S0263034618000083 Published online by Cambridge University Press

with betatron frequency ω_β (Ghotra & Kant, 2016*a*). The betatron oscillation frequency can be related from the transverse motion of electron, where $\omega_\beta = \sqrt{ev_z B_0/\gamma m_0 r_0 c}$. With $\omega_L = \omega_0\ (1 - v_z/v_{ph})$ the resonance condition is $eB_0/m_0 r_0 \omega_0^2 = (\gamma c/v_z)(1 - v_z/v_{ph})^2$. Thus, the different TEM mode indices affect the resonance. In Figure 1a, the resonance appears at normalized axial magnetic field $b_0 = 0.06$ where the electron energy gain is maximum. The axial magnetic field strengthens the $\vec{v} \times \vec{B}$ force experienced by the electron, and hence contributes significantly for enhancing electron energy gain for a trapped electron. The observed energy gain of about 100MeV, with $a_0 = 5$ at $r'_0 = 300$ without magnetic field is increased to 250MeV with axial magnetic field of 6MG (corresponds to normalized value $b_0 = 0.06$). Thus, the higher energy gain appears at a particular value of axial magnetic field. Liu *et al.* (2004) investigated that a strong magnetic field of the order of 100MG is required to accelerate a rest electron to a few MeV of energy with an intense laser pulse of peak intensity 2×10^{19}W/cm^2. In our model, the axial magnetic field under 6MG is sufficient to accelerate electron to a few 100MeV of energy using a (0, 1) mode of a CP–HG laser pulse of peak intensity 6.92×10^{19}W/cm^2. The energy gain is comparatively higher under the influence of axial magnetic field than without axial magnetic field for intensity parameter $a_0 = 25$ as depicted in Figure 1b. With $b_0 = 0.06$ and $r'_0 = 450$, the observed value is almost double with magnetic field than that without magnetic field. The axial magnetic field has been optimized for a set of laser parameters. This optimization is solely a base for maximum energy gained by the electron during interaction with a CP–HG laser pulse.

Figure 2 shows the electron trajectories with laser intensity parameter $a_0 = 5$ at $r'_0 = 150$ with and without optimized magnetic field. In Figure 2a, a de-phased electron trajectory appears in the absence of axial magnetic field. A phased electron trajectory with an inefficient acceleration appears in Figure 2b with a smaller magnetic field $b_0 = 0.006$ (0.64MG). An effective acceleration of electron appears with an optimized magnetic field, $b_0 =$ 0.06 (6.4MG) as depicted in Figure 2c. As appearing in Figure 2a without magnetic field, the scattering of electron goes on increasing with the propagation distance, whereas it is much reduced due to an axially applied magnetic field as depicted in Figure 2b. As per Figure 2c, more reduction in the scattering of electron is observed with optimized magnetic field $b_0 = 0.06$. Saberi & Maraghechi (2015) proposed that the optimized magnetic field parameter enforces the trapping of electron at the focus of laser pulse for stronger cyclotron resonance. Due to which the electron accelerated effectively with high energy gain. Dai *et al.* (2011) reported that the transverse component of electric field deflects the electron away from the beam axis when injected in the path of laser pulse. In our model, such deflection of electron away from the beam axis is controlled by using a smaller and optimized magnetic field along the longitudinal axis of a HG laser beam. The employed magnetic field is almost ten times smaller in comparison with the magnetic field stated by Liu *et al.* (2004) for laser magnetic resonance acceleration mechanism. The axial magnetic field can hold the accelerated electron around the axis of propagation of laser pulse due to cyclotron rotation (Akou & Hamedi, 2015). Thus, the optimized axial magnetic field supports effective acceleration of electron. The axial magnetic field is highly

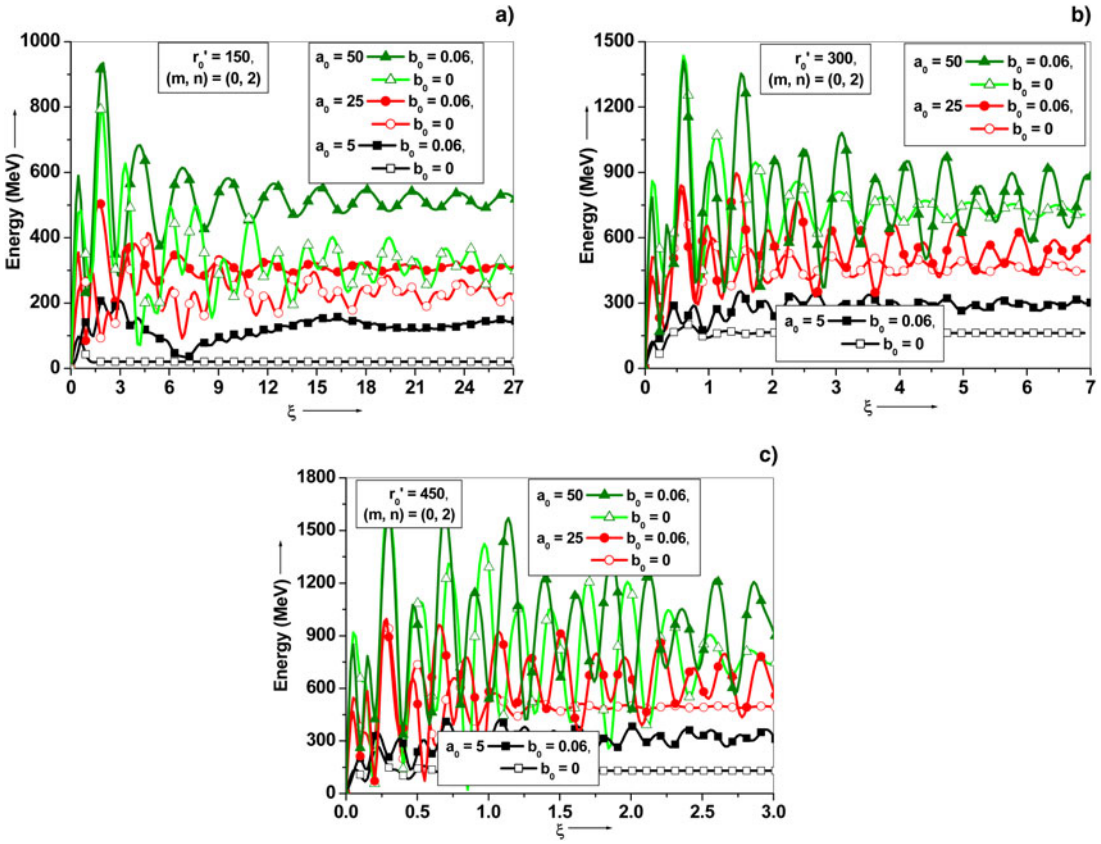

Fig. 4. Electron energy gain variations for $(m, n) = (0, 2)$ with a normalized function of propagation distance ξ for $b_0 = 0$ and $b_0 = 0.06$ and the intensity parameters $a_0 = 5$, 25, and 50 for (a) $r'_0 = 150$, (b) $r'_0 = 300$, and (c) $r'_0 = 450$. The other parameters are $\tau'_L = 70$, $\phi_0 = 0$, $p'_0 = 1$, $z'_L = 0$, $x'_i = 0$, $y'_i = 0$, and $z'_i = 0$.

https://doi.org/10.1017/S0263034618000083 Published online by Cambridge University Press

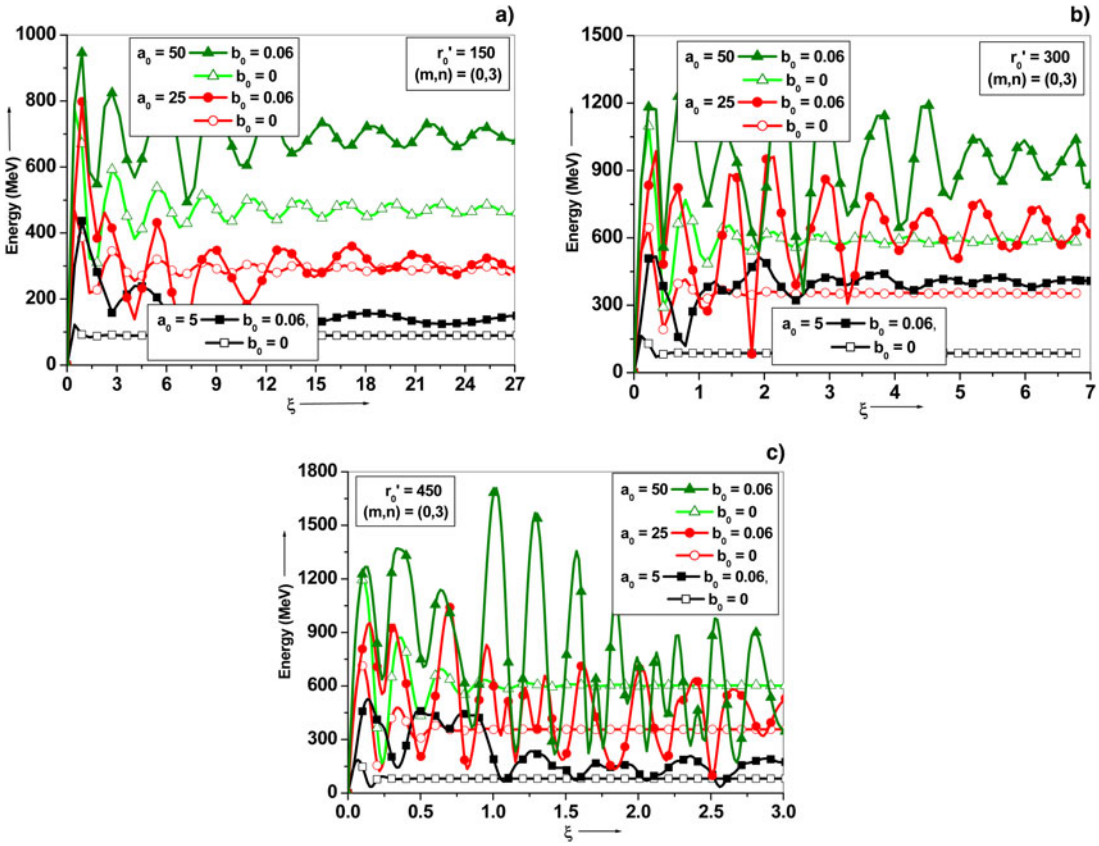

Fig. 5. Electron energy gain variations for $(m, n) = (0, 3)$ with a normalized function of propagation distance ξ for $b_0 = 0$ and $b_0 = 0.06$ and the intensity parameters as: $a_0 = 5$, 25, and 50 at (a) $r'_0 = 150$, (b) $r'_0 = 300$, and (c) $r'_0 = 450$. The other parameters are $\tau'_L = 70$, $\phi_0 = 0$, $p'_0 = 1$, $z'_L = 0$, $x'_i = 0$, $y'_i = 0$, and $z'_i = 0$.

supportive in controlling the electron that is going out of phase with the saturation of betatron resonance. Figure 2c presents a confined trajectory of electron orbit for a set of optimized parameters during laser–electron interaction.

Figure 3 represents the electron energy gain variations for the mode $(m, n) = (0, 1)$ with a normalized function of propagation distance ξ. The graphs have been plotted with distinct intensity parameters a_0 and laser spot sizes r'_0 in the absence and presence of magnetic field. Electron energy gain remains high for the higher intensity parameter with the same spot size. Figure 3a depicts electron energy gain of about 600MeV with $r'_0 = 150$ and $a_0 = 50$. Hartemann *et al.* (1995) analyzed the role played by a beam focus for attaining a high energy gained by an accelerating particle. The beam width parameter influences the accelerating distance expressed in terms of Rayleigh length with a Gaussian beam. The plots also show the variation of beam width function $f(\xi)$ with an increasing normalized propagation distance. The laser's beam width increases as the laser pulse propagates through the vacuum. For the smaller value of beam width parameter, stronger electron acceleration is depicted and *vice versa*. Thus, an effective electron energy gain is seen with a smaller value of beam width parameter at a small distance. The acceleration of electron appear due to the asymmetry in the intensity distribution of a CP–HG laser beam. It ensures the electron trapping, acceleration, and energy gain during the interaction with the leading part of the laser pulse where the electron first gains high energy. This energy gain almost saturates while reaching to the trailing end of the pulse. The calculated acceleration distance with a LP-chirped laser pulse for electron energy gain is almost three times the Rayleigh length with a large spot size $r'_0 = 900$ in vacuum (Ghotra & Kant, 2015*b*). The observed acceleration distance is about six times higher the Rayleigh length for a CP–HG laser pulse with a smaller initial laser spot size, $r'_0 = 300$ as depicted from Figure 3b. Figure 3c shows the electron energy gain with a larger spot size. Initially, the electron gains high energy from laser fields and soon after decelerated at larger propagation distance where the weakening of laser field appears. The electron is accelerated where laser field strength is high and decelerated with energy loss where field strength is low. This makes an efficient acceleration of electron. However, the deceleration appears smaller as it is controlled with the externally applied axial magnetic field. Hence, a comparative higher electron energy gain is observed in the presence of axial magnetic field than that without any additional magnetic field.

Figure 4 represents the electron energy gain variations without and with magnetic field as a function of ξ for the mode index $(m, n) = (0, 2)$ with different intensity parameters $a = 5$, 25, 50 and at different values of laser spot size: (a) $r'_0 = 150$, (b) $r'_0 = 300$, and (c) $r'_0 = 450$. Electron attains the maximum energy gain at shorter distance for higher values of intensity and decelerated with lower values of intensity and then saturates for longer distance. The deceleration remains smaller in the presence of axial magnetic field. The electron retains significant amount of energy at longer distance with magnetic field even in the presence of a weak laser field as depicted in Figures 4a–4c.

Figure 5 represents the electron energy gain variations without and with magnetic field as a function of ξ for the mode index $(m, n) = (0, 3)$ with different spot size and intensity parameters.

https://doi.org/10.1017/S0263034618000083 Published online by Cambridge University Press

In Figures 5b and 5c, the variation has been plotted for $r'_0 = 300$ and 450. The electron energy gain in the range of GeV is observed with laser intensity $I \sim 6.8 \times 10^{21}$W/cm^2 (for $a_0 = 50$) and spot size $r'_0 = 300$. Higher electron energy gain of about $\sim$ 1.65GeV is observed for $r'_0 = 150$ with the same intensity ($a_0 = 50$) as depicted in Figure 5c). The calculated accelerating distance is about three times the Rayleigh length in this case. It is also shown that the electron gains higher energy quickly with the higher mode indices in vacuum but retains only a smaller portion of gained energy for larger propagation distance in the absence of magnetic field. However, in the presence of magnetic field, it retains higher energy for longer distances. The intensity variations with higher mode indices report a weak field at larger propagation distance. Thus, with higher modes, the electron is unable to retain its gained energy for the larger propagation distances. Such loss is controlled when external magnetic field is applied. Thus, the energy loss under the influence of external applied axial magnetic field is comparatively smaller than that without magnetic field.

Figure 6 shows the electron energy gain without and with magnetic field as a function of laser peak power for mode indices $(m, n) = (0, 1)$ and $(0, 4)$. The observed electron energy gain increases with increase in laser peak power. The energy gained by the electron is above 1.5GeV at a peak power of about 10PW with mode index (0, 4), whereas it is about 0.5GeV with mode index (0, 1) in the absence of magnetic field in vacuum. The electron energy gain is above 2GeV at a peak power of 10PW with mode index (0, 4) in the presence of magnetic field in vacuum. Such high-energy PW class of lasers is feasible experimentally. The configuration of the hybrid amplification of 2×10PW femtosecond laser system of the Extreme Light Infrastructure – Nuclear Physics (ELI-NP) facility is described (Dabu, 2017). The depicted gain with magnetic field is about 30% higher than that without magnetic field. Thus, the electron energy gain is appeared sensitive to laser power and mode indices, it increases with increasing the mode index for the same magnitude of laser power for HG laser beam. An electron energy gain of about 262MeV was observed with a CP Gaussian laser pulse of peak intensity $\sim 10^{20}$W/cm^2 (Niu *et al.*, 2008). However, in our case, the observed energy gain is much higher when the higher mode index has been investigated with the same intensity than that with lower mode index for CP–HG laser pulse. Magnetic field above 10MG was considered with a CP Gaussian laser beam to attain energy gain above 100MeV (Sharma & Tripathi, 2009; Gupta & Ryu, 2005). In our study of electron acceleration with a mode index influenced CP–HG laser beams shows the higher energy gain in GeV range with a much smaller magnetic field of about 6.4MG even for mode index (0, 2).

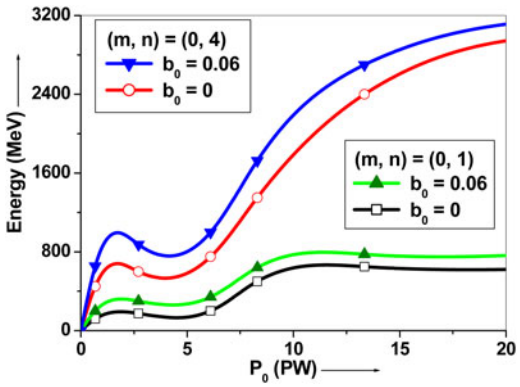

Fig. 6. Evolution of electron energy gain with laser peak power for $b_0 = 0$ and $b_0 = 0.06$ and the mode indices $(m, n) = (0, 1)$ and $(0, 4)$. The other parameters are same as referred in Figure 3.

Conclusion

The influence of intensity and power distribution in distinct TEM modes of HG laser on DLA of electron under the influence of axial magnetic field has been highlighted in this study. The role of laser beam width parameter has been reported for electron acceleration using a CP–HG laser beam. Using laser intensity $a_0 = 25$ ($I \sim 8.5 \times 10^{20}$W/cm^2) and laser spot size $r'_0 = 150$ ($\sim 25\mu$m) for mode (0, 4), electron energy gain of above 1GeV is observed due to externally applied axial magnetic field. The laser peak power for such case is calculated as 8.3PW. Though, the electron energy gain for higher modes is high, but it suffers with de-phasing of electron at shorter distance in the absence of any additional magnetic field. The applied magnetic field of about 6.4MG restricts such dephasing even with a laser intensity of about 10^{20}W/cm^2. About 30% higher electron energy gain is observed with magnetic field than that without magnetic field. With a suitable selection of laser parameters such as intensity, beam spot size, mode index, and optimized magnetic field, the electron is accelerated up to the order of GeV energy. The role of distinct mode indices under the influence of axial magnetic field can be utilized for the formulation of desired-sized accelerators based on the accelerating distance of electron. Thus, the obtained results with distinct TEM modes with the role of magnetic field will be helpful in the development of better table-top accelerators of diverse needs.

Acknowledgments. This work was supported by the UK Engineering and Physical Sciences Research Council (EPSRC) grants EP/J018171/1, EP/J500094/1 and EP/N028694/1, and the EC H2020 LASERLAB-EUROPE (grant no. 654148) and EuPRAXIA (grant no. 653782). This research was also supported in part by the International Centre for Theoretical Sciences (ICTS) during a visit for participating in the program – Laser Plasma Accelerator (Code: ICTS/Prog-LPA/2017/3).

References

Akou H and Hamedi M (2015) High energy micro electron beam generation using chirped laser pulse in the presence of an axial magnetic field. *Physics of Plasmas* **22**, 103120.

Albert F, Lemos N, Shaw JL, Pollock BB, Goyon C, Schumaker W, Saunders AM, Marsh KA, Pak A, Ralph JE, Martins JL, Amorim LD, Falcone RW, Glenzer SH, Moody JD and Joshi C (2017) Observation of betatron X-ray radiation in a self-modulated laser wake field accelerator driven with picosecond laser pulses. *Physical Review Letters* **118**, 134801 (1–5).

Dabu R (2017) High power, high contrast hybrid femtosecond laser systems. *AIP Conference Proceedings* **1852**, 070001(1–9).

Dai L, Li JX, Zang WP and Tian JG (2011) Vacuum electron acceleration driven by a tightly focused radially polarized Gaussian beam. *Optics Express* **19**(10), 9303.

Flacco A, Vieira J, Lifschitz A, Sylla F, Kahaly S, Veltcheva M, Silva LO and Malka V (2015) Persistence of magnetic field driven by relativistic electrons in plasma. *Nature Physics* **11**, 409–413.

Fortin PL, Piche M and Varin C (2010) Direct-field electron acceleration with ultrafast radially polarized laser beams: scaling laws and optimization. *Journal of Physics B: Atomic, Molecular and Optical Physics* **43**, 025401.

Geddes CGR, Toth C, Tilborg JV, Esarey E, Schroeder CB, Bruhwiler D, Nieter C, Cary J and Leemans WP (2004) High-quality electron beams

https://doi.org/10.1017/S0263034618000083 Published online by Cambridge University Press

from a laser wakefield accelerator using plasma-channel guiding. *Nature* **431**, 438–441.

Ghotra HS and Kant N (2015*a*) Electron acceleration to GeV energy by a chirped laser pulse in vacuum in the presence of azimuthal magnetic field. *Applied Physics B* **120**(1), 141–147.

Ghotra HS and Kant N (2015*b*) Electron acceleration by a chirped laser pulse in vacuum under influence of magnetic field. *Optical Review* **22**(4), 539–543.

Ghotra HS and Kant N (2016*a*) Polarization effect of a Gaussian laser pulse on magnetic field influenced electron acceleration in vacuum. *Optics Communications* **365**, 231–236.

Ghotra HS and Kant N (2016*b*) TEM modes influenced electron acceleration by Hermite–Gaussian laser beam in plasma. *Laser and Particle Beams* **34** (3), 385–393.

Ghotra HS and Kant N (2017) GeV electron acceleration by a Gaussian field laser with effects of beam width parameter in magnetized plasma. *Optics Communications* **383**, 169–176.

Gu YJ, Yu Q, Klimo O, Esirkepov TZ, Bulanov SV, Weber S and Korn G (2016) Fast magnetic energy dissipation in relativistic plasma induced by high order laser modes. *High Power Laser Science and Engineering* **4**, e19 (1–5).

Gupta DN and Ryu CM (2005) Electron acceleration by a circularly polarized laser pulse in the presence of an obliquely incident magnetic field in vacuum. *Physics of Plasmas* **12**, 053103(1–5).

Hartemann FV, Fochs SN, Sage GPL, Luhmann Jr NC, Woodworth JG, Perry MD, Chen YJ and Kerman AK (1995) Nonlinear ponderomotive scattering of relativistic electrons by an intense laser field at focus. *Physical Review E* **51**, 4833–4843.

Joshi C (2007) The development of laser- and beam-driven plasma accelerators as an experimental field. *Physics of Plasmas* **14**, 055501.

Kawata S, Kong Q, Miyazaki S, Miyauchi K, Sonobe R, Sakai K, Nakajima K, Masuda S, Ho YK, Miyanaga N, Limpouch J and Andreev AA (2005) Electron bunch acceleration and trapping by the ponderomotive force of an intense short-pulse laser. *Laser and Particle Beams* **23**, 61–67.

Leemans WP, Nagler B, Gonsalves AJ, Toth C, Nakamura K, Geddes CGR, Esarey E, Schroeder CB and Hooker SM (2006) GeV electron beams from a centimetre-scale accelerator. *Nature Physics* **2**, 696–699.

Liu H, He XT and Chen SG (2004) Resonance acceleration of electrons in combined strong magnetic fields and intense laser fields. *Physical Review E* **69**, 066409.

Malka V, Faur J, Gauduel YA, Lefebvre E, Rousse A and Phuoc KT (2008) Principles and applications of compact laser–plasma accelerators. *Nature Physics* **4**, 447.

Mohammed J, Ghotra HS, Kaur R, Hafeez HY and Kant N (2017) Electron acceleration in Bubble Regime. *AIP Conference Proceedings* **1860**, 020013 (1–7).

Nakatsutsumi M, Sentoku Y, Korzhimanov A, Chen SN, Buffechoux S, Kon A, Atherton B, Audebert P, Geissel M, Hurd L, Kimmel M, Rambo P, Schollmeier M, Schwarz J, Starodubtsev M, Gremillet L, Kodama R and Fuchs J (2018) Self-generated surface magnetic fields inhibit laser driven sheath acceleration of high-energy protons. *Nature Communications* **9**, 280.

Niu HY, He XT, Qiao B and Zhou CT (2008) Resonant acceleration of electrons by intense circularly polarized Gaussian laser pulse. *Laser and Particle Beams* **26**, 51–59.

Robinson APL, Arefiev AV and Neely D (2013) Generating "superponderomotive" electrons due to a non-wake-field interaction between a laser pulse and a longitudinal electric field. *Physical Review Letters* **111**, 065002.

Saberi H and Maraghechi B (2015) Enhancement of electron energy during vacuum laser acceleration in an inhomogeneous magnetic field. *Physics of Plasmas* **22**, 033115(1–5).

Salamin YI (2017) Electron acceleration in vacuum by a linearly-polarized ultra-short tightly-focused THz pulse. *Physics Letters A* **381**(18), 3010–3013.

Sharma A and Tripathi VK (2009) Ponderomotive acceleration of electrons by a laser pulse in magnetized plasma. *Physics of Plasmas* **16**, 043103(1–5).

Spinka TM and Haefner C (2017) High-average-power ultrafast lasers. *Optics & Photonics* **10**, 26–33.

Sprangle P, Esarey E and Krall J (1996) Laser driven electron acceleration in vacuum, plasma, and gases. *Physics of Plasmas* **3**(5), 2183–2190.

Tajima T and Dawson JM (1979) Laser electron accelerator. *Physical Review Letters* **43**, 267.

Umstadter D (2003) Relativistic laser-plasma interactions. *Journal of Physics D: Applied Physics* **36**, R151.

Wallin E, Gonoskov A, Harvey C, Lundh O and Marklund M (2017) Ultraintense laser pulses in near-critical underdense plasmas-radiation reaction and energy partitioning. *Journal of Plasma Physics* **83**, 905830208(1–13).

Xiao KD, Huang TW, Ju LB, Li R, Yang SI, Yang YC, Wu SZ, Zhang H, Qiao B, Ruan SC, Zhou CT and He XT (2016) Energetic electron-bunch generation in a phase-locked longitudinal laser electric field. *Physical Review E* **93**, 043207.

https://doi.org/10.1017/S0263034618000083 Published online by Cambridge University Press